Robotica (2002) volume 20, pp. 81–91. © 2002 Cambridge University Press
DOI: 10.1017/S0263574701003654 Printed in the United Kingdom

Mechanism design of a simplified 6-DOF 6-RUS parallel manipulator

Xin-Jun Liu*[a], Jinsong Wang*, Feng Gao** and Li-Ping Wang*

(Received in Final Form: June, 2, 2001)

SUMMARY
This paper concerns the issue of mechanism design of a simplified 6-DOF 6-RUS parallel manipulator. The design of robotic mechanisms, especially for 6-DOF parallel manipulators, is an important and challenging problem in the field of robotics. This paper presents a design method for robotic mechanisms, which is based on the physical model of the solution space. The physical model of the solution space, which can transfer a multi-dimensional problem to a two or three-dimensional one, is a useful tool to obtain all kinds of performance atlases. In this paper, the physical model of the solution space for spatial 6-RUS (R stands for revolute joint, U universal joint and S spherical joint) parallel manipulators is established. The atlases of performances, such as workspace and global conditioning index, are plotted in the physical model of the solution space. The atlases are useful for the mechanism design of the 6-RUS parallel manipulators. The technique used in this paper can be applied to the design of other robots.

KEYWORDS: Parallel manipulators; Mechanism design; Physical model of solution space; Workspace; Global conditioning index.

1. INTRODUCTION

The design of robotic mechanisms is an important and challenging problem in the field of robotics. Two issues are involved in the optimal design of robot: performance evaluation and synthesis. Having designed a robot, it is necessary to evaluate its main characteristics. A second problem is to determine the dimensions (link lengths) of the robot, which are the most suitable for the task at hand. The latter one is one of the most difficult issues in the field of robotics.

As is well known, the performances of parallel robots heavily depend upon their dimensions. Therefore, the process of mechanism design for a manipulator is based largely on the use of some criteria, such as workspace,[1,2] dexterity,[3,4] payload,[5] conditioning index,[6,7] and stiffness.[8]

The classical methods of design, such as the cost-function approach, experience difficulties in dealing with this problem.[9] The first difficulty is due to the large number of parameters that are involved. For example, a generic 6-DOF serial manipulator can have as many as 18 geometric parameters, 60 mass parameters, and 42 stiffness parameters along with 12 or more actuator parameters.[10] The second one is that the cost function may have numerous local minima and, consequently, the minimization procedure may have difficulties in locating the global minima. Another drawback of the method is that it cannot obtain the most optimal design parameters, for example, the link lengths of the robots.

The link lengths of robotic mechanisms can be measured by various units and can be changed between zero and infinity. So that, it is of primary importance to develop a useful design tool that can express the relationships between criteria and link lengths of robots. From papers,[5,7,11] we can see that the physical model of the solution space of robotic mechanisms is a useful one. The design tool is a tool that all non-dimensional link lengths of robots are embodied in a finite space. The relationships between criteria and link lengths of all robots can be plotted in the physical model of the solution space, and then the atlases are obtained. Based on the performance atlases, we can select most optimal group of link lengths for manipulators.

In this paper, the method mentioned above is applied to the design of simplified 6-DOF 6-RUS parallel manipulators. A physical model of the solution space for the robotic mechanisms is established. The atlases of criteria, such as workspace, global conditioning index, global velocity index and global payload index, are plotted in the physical model of the solution space. The atlases are useful for design of the simplified 6-DOF 6-RUS parallel manipulators. The technique used in this paper can be applied to the design of other manipulators.

2. THE DESIGN METHOD

The performances of parallel robots are heavily dependent on the dimensions of manipulators. Therefore, it is important to design link lengths of manipulators with respect to performances, which will be the most suitable for the task at hand. Theoretically, since link lengths of robotic mechanisms may vary between zero and infinity, which means that the links can be very long or short and can be measured by different units, it is very difficult to investigate the relationships between performance criteria and link lengths of all robotic mechanisms. Therefore, it is convenient to eliminate the physical sizes of mechanisms.

* Manufacturing Engineering Institute, Department of Precision Instruments, Tsinghua University, Beijing, 100084 (P.R. of China)
** Robotics Research Center, Hebei University of Technology, Tianjin, 300130 (P.R. of China).
[a] Corresponding Author E-mail: liuxj@post.pim.tsinghua.edu.cn or xinjunl@yahoo.com

In 1985, a novel design space, called physical model of the solution space, for planar 4-bar mechanisms was proposed by Yang and Gao.[11] The coordinates of the design space are characterized by the non-dimensional link lengths of the generalized planar 4-bar mechanisms, each of which is the link length divided by the sum of four link lengths. Because there are one-to-one corresponding relationships between the points in the physical model of the solution space and the planar 4-bar mechanisms, the solution space can be used to establish the relationships between the performance criteria and all the mechanisms.

In the fieid of design for robotic mechanisms, one common method is to establish objective functions subject to specified conditions. Generally, the objective functions are multielement, so that the method cannot solve the general problems. Mostly, robots have not been designed to perform specific tasks but to meet general performance criteria. As mentioned earlier, the physical model of the solution space is a design space that can contain all the non-dimensional mechanisms. And the relationships between the performance criteria and the link lengths of mechanisms can be illustrated in this space. Using the physical model of the solution space, some important results are obtained for the design of the manipulators.[5,7,11]

In fact, the physical model of the solution space is a global non-dimensional link lengths space for mechanisms. It is a tool to transfer the problems from the multi-dimensional design space to a two- or three-dimensional one. In this way, we can solve the problem of decreasing the design parameters of parallel manipulators in the field of design for manipulators. When we characterize the performance by contours in the physical model of the solution space of manipulators, atlases are generated. The atlases are the guidelines to optimize the structural parameters from all groups of link lengths of the manipulators.

In the following sections, the design method is applied to the design of simplified 6-DOF 6-RUS parallel manipulators. The atlases of workspace and global conditioning index are plotted in the physical model of the solution space. The atlases are useful for the mechanism design of the parallel manipulators. The design results of the manipulators are obtained.

3. PHYSICAL MODEL OF THE SOLUTION SPACE FOR SIMPLIFIED 6-DOF 6-RUS PARALLEL MANIPULATORS

Parallel robots are characterized by higher stiffness, payload, accuracy, etc., than serial robots, to which many researchers have paid attention. In the family of parallel manipulators, the 6-UPS Stewart platform is a famous one. The platform mechanisms have been introduced by Gough and were later on used by Stewart[12] as early models of flight simulators. The first design of a manipulator system was done by MacCallion and Pham[13] for an assembly workstation. Now this type of kinematic structure seems to be widely accepted for the design of commercially used flight simulators. Most of the research on this platform mechanism was devoted to the kinematic and dynamic analysis as well as the development of control strategies.[14–17]

The spatial in-parallel actuated 6-RUS (or 6-RSS) manipulators have attracted many researchers' attention in the past decade.[18–24] The manipulator can be applied to the fields of machine tools,[20] 6-Axis positioners,[18] and motion simulators.[23] The simplified 6-DOF 6-RUS parallel manipulator considered in this paper, is shown in Figure l(a), which consists of two rigid bodies connected by six legs OB_iP_i (i = 1, 2, . . . , 6). The stationary rigid body is referred to as the base and the moving rigid body is referred to as the mobile platform. The center of the universal joint connecting the *i*th leg to the link linking to the base will be denoted as B_i whereas the center of the spherical joint connecting the same leg to the platform will be denoted as P_i. Each leg of the manipulator connects to the base through a revolute joint, whose center is denoted as *O*. Vectors $\boldsymbol{p}_i$ (i = 1, . . . , 6) will be defined as the position vectors of the platform joints, vectors $\boldsymbol{b}_i$ (i = l, . . . , 6) will be defined as the position vectors of the universal joints. The geometric parameters of the manipulator are $O'P_i = R_3$, $P_iB_i = R_2$, $OB_i = R_1$ and the angle ϕ as shown in Figure 1(b). Let,

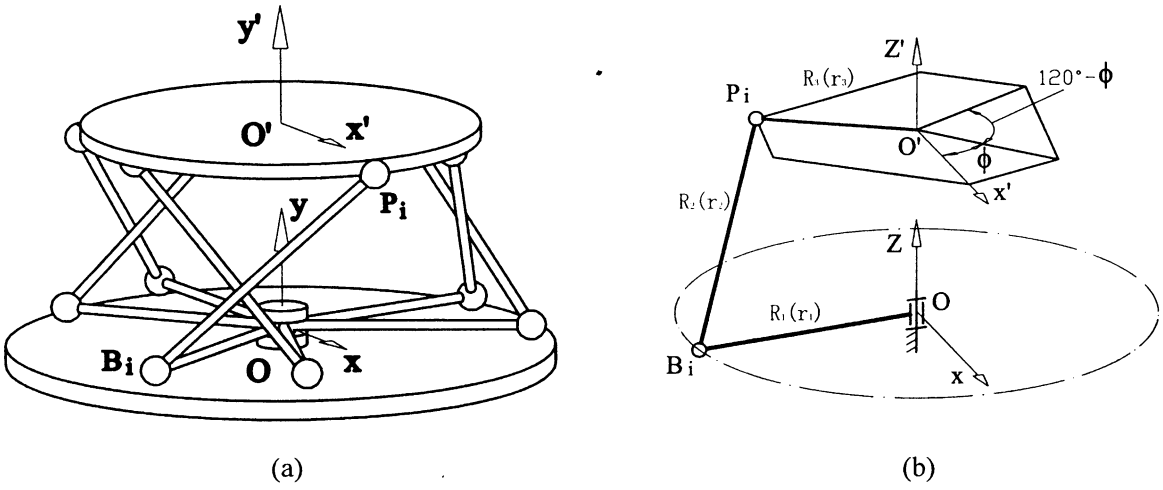

Fig. 1. The geometric architecture of 6-DOF 6-RUS Parallel Manipulators.

https://doi.org/10.1017/S0263574701003654 Published online by Cambridge University Press

$$r_i = R_i / L, \quad i = 1, 2, 3 \tag{1}$$

where

$$L = \frac{R_1 + R_2 + R_3}{3} \tag{2}$$

Then

$$r_1 + r_2 + r_3 = 3 \tag{3}$$

which means that anyone of r_1, r_2 and r_3 can reach the maximum value 3. But, if $r_1 > 1.5$ or $r_3 > 1.5$, there is $r_2 + r_3 < 1.5$ or $r_2 + r_1 < 1.5$, which means that the manipulator cannot be assembled. Therefore, there must be

$$r_1, r_3 < 1.5, r_2 < 3 \tag{4}$$

The physical model of the solution space of the manipulators can be obtained as illustrated in the parallelogram *ABCD* in Figure 2. The planar closed-configuration of the solution space is shown in Figure 3. All non-dimensional simplified 6-DOF 6-RUS parallel manipulators are within the physical model of the solution space.

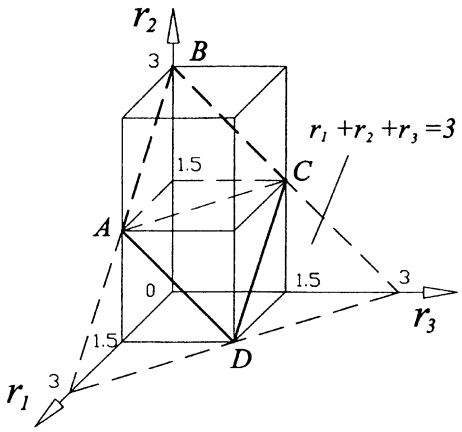

Fig. 2. The physical model of the solution space of 6-RUS Parallel Manipulators.

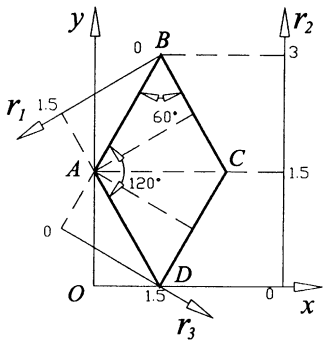

Fig. 3. The planar-closed configuration.

4. THE INVERSE KINEMATIC PROBLEM

Let us consider a fixed coordinate frame $\boldsymbol{R}: O - xyz$ attached to the base of the manipulator and a mobile coordinate frame $\boldsymbol{R}': O' - x'\,y'\,z'$ attached to the platform, where O' is the point to be positioned by the manipulator, and the position of point O' with respect to the fixed frame $\boldsymbol{R}$ is denoted as vector

$$\boldsymbol{r}_R = [x, y, z]^T \tag{5}$$

where x, y and z are non-dimensional variables, respectively. Furthermore, let $\boldsymbol{Q}$ be the rotation matrix describing the orientation of $\boldsymbol{R}'$ with respect to $\boldsymbol{R}$. The matrix can be expressed by three angles noted as ϕ_1, ϕ_2 and ϕ_3, respectively, as follows

$$\boldsymbol{Q} = \begin{bmatrix} q_{11} & q_{12} & q_{13} \\ q_{21} & q_{22} & q_{23} \\ q_{31} & q_{32} & q_{33} \end{bmatrix} \tag{6}$$

where

$$\begin{aligned}
q_{11} &= -\sin\phi_1 \sin\phi_3 + \cos\phi_1 \cos\phi_3 \cos\phi_2 \\
q_{12} &= -\sin\phi_1 \cos\phi_3 - \cos\phi_1 \sin\phi_3 \cos\phi_2 \\
q_{13} &= \cos\phi_1 \sin\phi_2 \\
q_{21} &= \cos\phi_1 \sin\phi_3 + \sin\phi_1 \cos\phi_3 \cos\phi_2 \\
q_{22} &= \cos\phi_1 \cos\phi_3 - \sin\phi_1 \sin\phi_3 \cos\phi_2 \\
q_{23} &= \sin\phi_1 \sin\phi_2 \\
q_{31} &= -\cos\phi_3 \sin\phi_2 \\
q_{32} &= \sin\phi_3 \sin\phi_2 \\
q_{33} &= \cos\phi_2
\end{aligned} \tag{7}$$

The vectors $\boldsymbol{P}_i$ in the fixed frame $\boldsymbol{R}$ can be written as

$$\boldsymbol{p}_{iR} = \boldsymbol{r}_R + \boldsymbol{Q}\boldsymbol{p}_{iR'} \quad i = 1, \ldots, 6 \tag{8}$$

where

$$\boldsymbol{p}_{iR'} = \begin{bmatrix} r_3 \cos\eta_i \\ r_3 \sin\eta_i \\ 0 \end{bmatrix} \quad i = 1, \ldots, 6 \tag{9}$$

and

$$\eta = \begin{bmatrix} \eta_1 \\ \eta_2 \\ \eta_3 \\ \eta_4 \\ \eta_5 \\ \eta_6 \end{bmatrix} = \begin{bmatrix} 0 \\ \phi \\ 2\pi/3 \\ 2\pi/3 + \phi \\ -2\pi/3 \\ \phi - 2\pi/3 \end{bmatrix} \tag{10}$$

As shown in Figure 1, the axes of the six revolute joints are aligned with the y-axis. Therefore, the vectors $\boldsymbol{b}_i$ in the fixed frame $\boldsymbol{R}$ can be written as

$$\boldsymbol{b}_{iR} = \begin{bmatrix} r_1 \cos\theta_i \\ r_1 \sin\theta_i \\ 0 \end{bmatrix} \quad i = 1, \ldots, 6 \tag{11}$$

https://doi.org/10.1017/S0263574701003654 Published online by Cambridge University Press

where θ_i is the actuated angle of the ith leg. Then the inverse kinematics problem of the manipulators can be solved by writing the following constraint equation

$$\| \boldsymbol{p}_{iR} - \boldsymbol{b}_{iR} \| = r_2 \quad i=1, \ldots, 6 \tag{12}$$

that is

$$\| \boldsymbol{r}_R + \boldsymbol{Q}\boldsymbol{p}_{iR'} - \boldsymbol{b}_{iR} \| = r_2 \quad i=1, \ldots, 6 \tag{13}$$

from which we can obtain

$$\theta_i = 2 \tan^{-1}(t_i) \tag{14}$$

where

$$t_i = \frac{-\nu_i \pm \sqrt{\nu_i^2 - 4u_i w_i}}{2u_i} \tag{15}$$

and

$$\begin{aligned} u_i &= r_1^2 + a_i^2 + b_i^2 + c_i^2 - r_2^2 + 2r_1 a_i \\ \nu_i &= -4r_1 b_i \\ w_i &= r_1^2 + a_i^2 + b_i^2 + c_i^2 - r_2^2 - 2r_1 a_i \\ a_i &= q_{11} r_3 \cos \eta_i + q_{12} r_3 \sin \eta_i + x \\ b_i &= q_{21} r_3 \cos \eta_i + q_{22} r_3 \sin \eta_i + y \\ c_i &= q_{31} r_3 \cos \eta_i + q_{32} r_3 \sin \eta_i + z \end{aligned}$$

Hence, for a given manipulator and for prescribed values of the position and orientation of the platform, the required actuated angles θ_i can be directly computed from Eq. (14). From Eq. (15), we can see that there are 2^6 branch sets for the manipulator under study. In this paper, the branch set as shown in Figure 1(a) is considered.

5. WORKSPACE AND ITS ATLASES

5.1. Geometric description of the constant-orientation workspace

Since the workspace of a 6-DOF parallel manipulator is embedded in a six-dimensional space, it is very difficult to represent. The constant-orientation workspace is the region of the three-dimensional Cartesian space that can be attained by a point from the platform of the manipulator for a given orientation of the platform. This is, in fact, a three-dimensional section of the six-dimensional complete workspace. The constant-orientation workspace of a 6-RUS parallel manipulator can be easily obtained geometrically[24] based on the inverse kinematic problem of the manipulator.

From Eq. (13), one can obtain

$$(x - x_i)^2 + (y - y_i)^2 + (z - z_i)^2 = r_2^2 \quad i=1, \ldots, 6 \tag{16}$$

where

$$x_i = r_i \cos \theta_i - q_{11} r_3 \cos \eta_i - q_{12} r_3 \sin \eta_i \tag{17}$$

$$y_i = r_1 \sin \theta_i - q_{21} r_3 \cos \eta_i - q_{22} r_3 \sin \eta_i \tag{18}$$

$$z_i = -q_{31} r_3 \cos \eta_i - q_{32} r_3 \sin \eta_i \tag{19}$$

from which we can see that Eq. (16) represents six spheres centered at the points $O_i(x_i, y_i, z_i)$ and the radius r_2. Let us consider Eqs. (17) and (18), which can be rewritten as

$$r_1 \cos \theta_i = x_i + x_{oi} \tag{20}$$

$$r_1 \sin \theta_i = y_i + y_{oi} \tag{21}$$

that is

$$(x_i + x_{oi})^2 + (y_i + y_{oi})^2 = r_1^2 \tag{22}$$

where

$$x_{oi} = q_{11} r_3 \cos \eta_i + q_{12} r_3 \sin \eta_i \tag{23}$$

$$y_{oi} = q_{21} r_3 \cos \eta_i + q_{22} r_3 \sin \eta_i \tag{24}$$

x_{oi} and y_{oi} are related to the value of η_i. When η_i is specified, the circle of Eq. (22) can be determined. The circle is centered at point $O_{Oi}(-x_{oi}, -y_{oi})$ and is with radius r_1. Therefore, the center of the sphere centered at point $O_i(x_i, y_i, z_i)$ is on the circle centered at $O_{Oi}(-x_{oi}, -y_{oi})$.

From the above analysis, we can see that the workspace of each of the six legs of a simplified 6-RUS manipulator is the enveloping solid of a sphere whose center is moved along a circle centered at point of $O_{Oi}(-x_{oi}, -y_{oi})$. The enveloping solid is a torus solid whose center is $O_{ti}(-x_{oi}, -y_{oi}, z_i)$. The constant-orientation workspace of a 6-RUS parallel manipulator is the intersection of six identical tori.[24] From Eqs. (16)–(18) and (23)–(24), one sees that the position vector of the center point $O_{ti}(-x_{oi}, -y_{oi}, z_i)$ is related to matrix $\boldsymbol{Q}$ and the position vectors $\boldsymbol{p}_{iR'}$ and $\boldsymbol{b}_{iR}$. For a given manipulator, the position vectors $\boldsymbol{p}_{iR'}$ and $\boldsymbol{b}_{iR}$ are constant. Hence, points $O_{ti}(-x_{oi}, -y_{oi}, z_i)$ are only related to the rotation matrix $\boldsymbol{Q}$. Therefore, if the orientation of the manipulator is specified, the constant-orientation workspace and its volume can be obtained geometrically by using Eqs. (16) and (22) using the commercial CAD system AutoCAD, for example.

As an example of application of the method described above, the workspace of a 6-RUS parallel manipulator, whose geometric parameters are $r_1 = 0.8$, $r_2 = 1.2$, $r_3 = l.0$ and $\phi = 0.0$, will now be studied. The constant-orientation workspace of the simplified 6-RUS parallel manipulator will be obtained, when $\boldsymbol{Q} = \boldsymbol{1}$, where $\boldsymbol{1}$ is the identity matrix. As mentioned previously, for the first leg, $i=1$, the workspace is a torus generated by the arc of *abcd* revolving with respect to the axis Z'', as shown in Figure 4(a). One-half of the torus is shown in Figure 4(b). The constant-orientation workspace of the manipulator is the intersection of six such tori, as shown in Figure 5. The volume of the workspace is $V = 4.65$, as obtained by AutoCAD.

In this paper, in the detennination of the constant-orientation workspace and reachable workspace, only the kinematic constraints are taken into account. Neither joint limits nor leg interference constraints are verified.

5.2. The reachable workspace and the atlases of volume

The constant-orientation workspace of a simplified 6-RUS parallel manipulator is determined geometrically. Although the reachable workspace is the union of all constant-orientation workspaces, its determination cannot be solved

https://doi.org/10.1017/S0263574701003654 Published online by Cambridge University Press

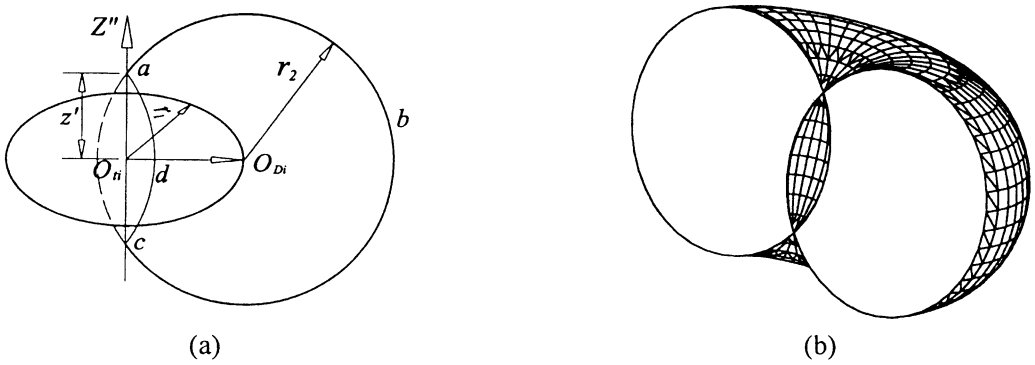

(a) (b)

Fig. 4. The workspace of each of legs is the torus generated by the closed arc *abcd* with respect to axis of Z''.

geometrically. Therefore, the reachable workspace can only be obtained numerically.

Using a numerical method, the volumes of the simplified 6-RUS parallel manipulators in the physical model of the solution space, as shown in Figure 3, can be obtained for a specified angular parameter ϕ. The corresponding atlases can be plotted as shown in Figure 6, from which we can see that:

- The volume in each of the atlases is inversely proportional to r_3, if r_1 is specified;
- If r_1 is specified, the volume is proportional to r_2;
- From Figure 6(a), (b) and (c), we can conclude that the volume of the reachable workspace for a simplified 6-RUS parallel manipulator, r_1, r_2 and r_3 being specified, changes little for various value of ϕ.

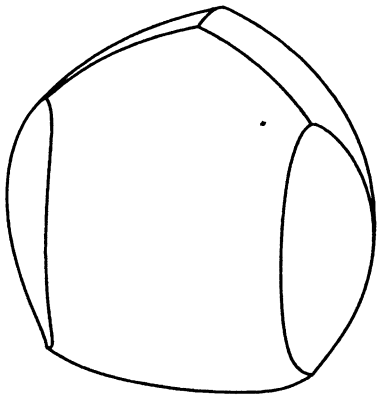

Fig. 5. The constant-orientation workspace of 6-RUS Parallel Manipulator.

5.3. The characteristics of workspace shape for simplified 6-RUS parallel manipulators

From the analysis of Section 5.1, we can see that if the non-dimensional parameters of a simplified 6-RUS parallel manipulator are subject to

$$r_2 > r_1 + r_3 \tag{25}$$

there is a void in the constant-orientation workspace of the manipulator, when $\boldsymbol{Q}=\mathbf{1}$. The planar-closed configuration of the physical model of the solution space is divided into two regions I and II with respect to the line

$$r_2 = r_1 + r_3 \tag{26}$$

Additionally, two lines

$$r_1 = r_2 \tag{27}$$

$$r_3 + 1.5 = r_2 \tag{28}$$

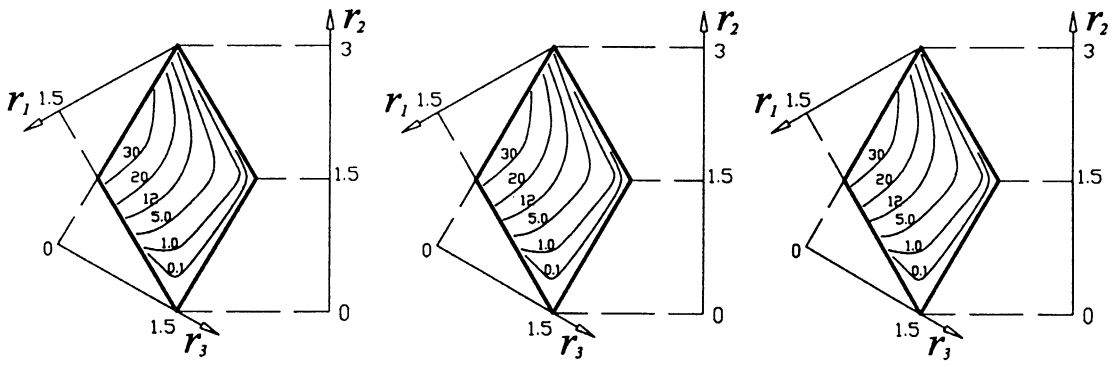

(a) $\phi = 0$ (b) $\phi = 30°$ (c) $\phi = 60°$

Fig. 6. Atlases of reachable workspace for 6-RUS Parallel Manipulators.

https://doi.org/10.1017/S0263574701003654 Published online by Cambridge University Press

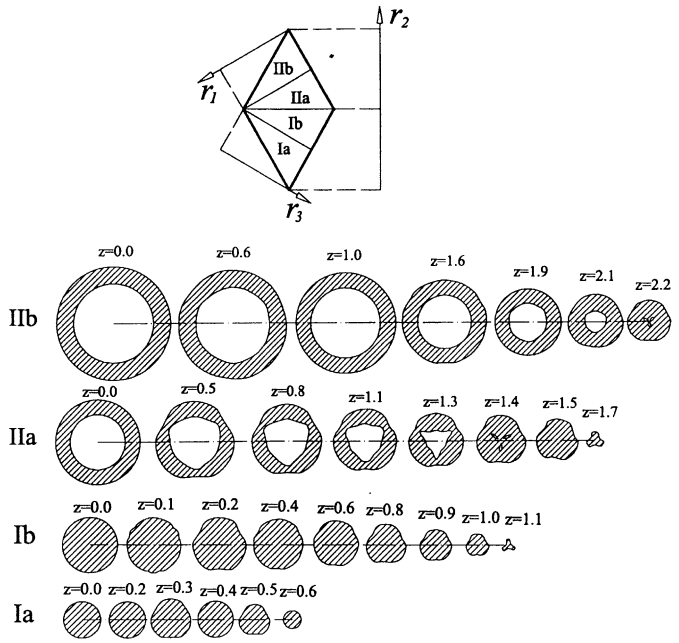

Fig. 7. Distribution of workspace shape in the physical model of the solution space for 6-RUS Manipulators.

are used, which divide the configuration into four sub-regions of Ia, Ib, IIa and IIb, as shown in Figure 7. Then the workspace for the manipulators (ϕ=30°) is classified into four types, and the distribution of the workspaces in the physical model of the solution space is illustrated in Figure 7. The workspaces are represented by several sections. From Figure 7, we can see that

- The workspaces of the simplified 6-RUS parallel manipulators in region I do not contain voids. If r_1 is specified, the workspace volume is inversely proportional to r_3;
- In region II, the workspaces of the manipulators contain voids. If r_1 is specified, the workspace volume is inversely pioportional to r_3.

6. ATLASES OF GLOBAL CONDITIONING INDICES

6.1. Jacobian matrix of simplified 6-RUS parallel manipulators

Differentiating Eq. (13) with respect to time and then rearranging terms leads to

$$d_i\dot{\theta}_i = e_i\dot{x} + f_i\dot{y} + g_i\dot{z} + l_i\dot{\phi}_1 + m_i\dot{\phi}_2 + n_i\dot{\phi}_3 \quad i = 1, \cdots, 6 \quad (29)$$

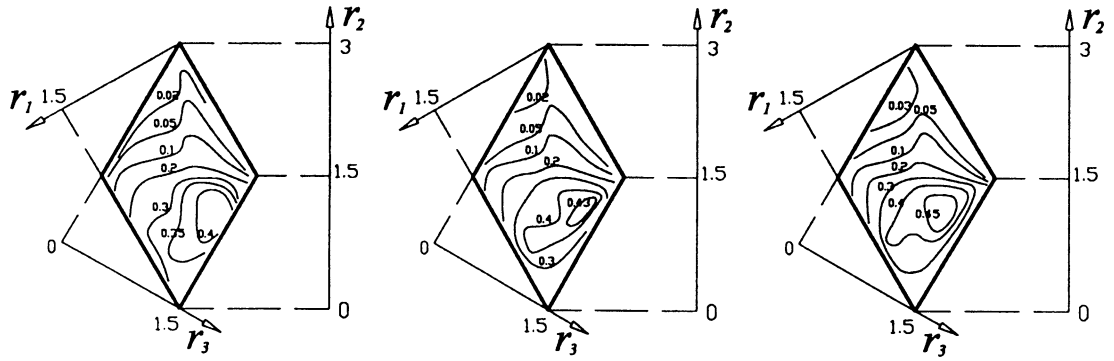

(a) $\phi = 0$ (b) $\phi = 30°$ (c) $\phi = 60°$

Fig. 8. Atlases of Global Linear Velocity Conditioning Index for 6-RUS Parallel Manipulators.

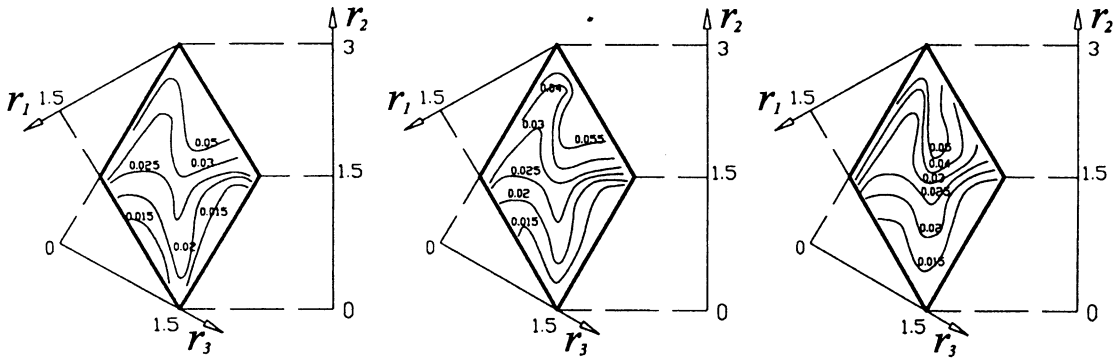

(a) $\phi = 0$ (b) $\phi = 30°$ (c) $\phi = 60°$

Fig. 9. Atlases of Global Angular Velocity Conditioning Index for 6-RUS Parallel Manipulators.

https://doi.org/10.1017/S0263574701003654 Published online by Cambridge University Press

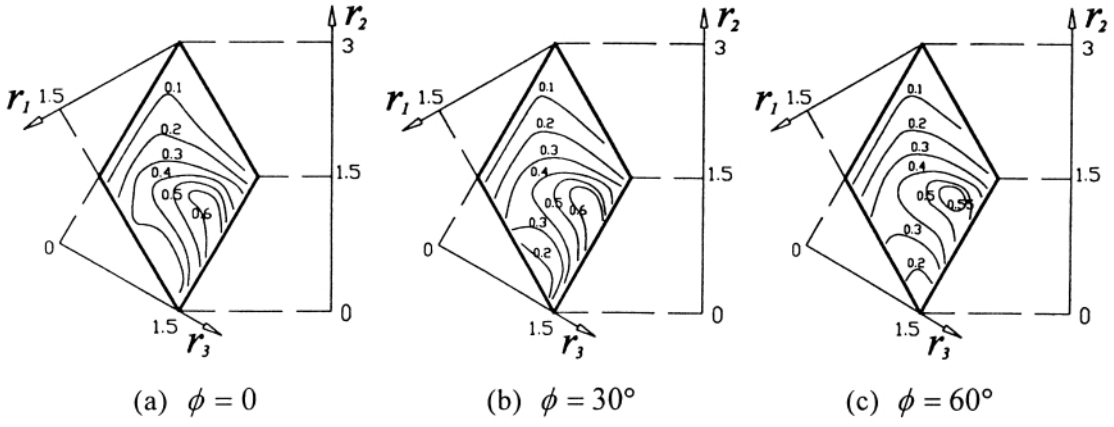

Fig. 10. Atlases of Global Force Conditioning Index for 6-RUS Parallel Manipulators.

where

$$
\begin{aligned}
d_i &= r_1 b_i \cos\theta_i - r_1 a_i \sin\theta_i \\
e_i &= a_i - r_1 \cos\theta_i \\
f_i &= b_i - r_1 \sin\theta_i \\
g_i &= c_i \\
l_i &= (a_i - r_1\cos\theta_i)(r_3\cos\eta_i q_{11a} + r_3\sin\eta_i q_{12a}) + \\
&\quad (b_i - r_1\sin\theta_i)(r_3\cos\eta_i q_{21a} + r_3\sin\eta_i q_{22a}) \\
m_i &= (a_i - r_1\cos\theta_i)(r_3\cos\eta_i q_{11b} + r_3\sin\eta_i q_{12b}) + \\
&\quad (b_i - r_1\sin\theta_i)(r_3\cos\eta_i q_{21b} + r_3\sin\eta_i q_{22b}) + \\
&\quad c_i(r_3\cos\eta_i q_{31b} + r_3\sin\eta_i q_{32b}) \\
n_i &= (a_i - r_1\cos\theta_i)(r_3\cos\eta_i q_{11c} + r_3\sin\eta_i q_{12c}) + \\
&\quad (b_i - r_1\sin\theta_i)(r_3\cos\eta_i q_{21c} + r_3\sin\eta_i q_{22c}) + \\
&\quad c_i(r_3\cos\eta_i q_{31c} + r_3\sin\eta_i q_{32c})
\end{aligned}
$$

and

$$
\begin{aligned}
q_{11a} &= q_{22c} = -\cos\phi_1\sin\phi_3 - \sin\phi_1\cos\phi_3\cos\phi_2 \\
q_{11b} &= -\cos\phi_1\cos\phi_3\sin\phi_2 \\
q_{11c} &= q_{22a} = -\sin\phi_1\cos\phi_3 - \cos\phi_1\sin\phi_3\cos\phi_2 \\
q_{12a} &= \sin\phi_1\sin\phi_3\cos\phi_2 - \cos\phi_1\cos\phi_3 \\
q_{12b} &= \cos\phi_1\sin\phi_3\sin\phi_2 \\
q_{12c} &= \sin\phi_1\sin\phi_3 - \cos\phi_1\cos\phi_3\cos\phi_2 \\
q_{21a} &= -q_{12c} \\
q_{21b} &= -\sin\phi_1\cos\phi_3\sin\phi_2 \\
q_{21c} &= -q_{12a} \\
q_{22b} &= \sin\phi_1\sin\phi_3\sin\phi_2 \\
q_{31b} &= -\cos\phi_3\cos\phi_2 \\
q_{31c} &= \sin\phi_3\sin\phi_2 \\
q_{32b} &= \sin\phi_3\cos\phi_2 \\
q_{32c} &= \cos\phi_3\sin\phi_2
\end{aligned}
$$

The kinematic equation of the manipulators can be written as

$$[\dot\theta_1\ \dot\theta_2\ \dot\theta_3\ \dot\theta_4\ \dot\theta_5\ \dot\theta_6]^T = \boldsymbol{K}[\dot x\ \dot y\ \dot z\ \dot\phi_1\ \dot\phi_2\ \dot\phi_3]^T \tag{30}$$

where

$$\boldsymbol{K} = \begin{bmatrix} e_1/d_1 & f_1/d_1 & g_1/d_1 & l_1/d_1 & m_1/d_1 & n_1/d_1 \\ \vdots & \vdots & \vdots & \vdots & \vdots & \vdots \\ e_6/d_6 & f_6/d_6 & g_6/d_6 & l_6/d_6 & m_6/d_6 & n_6/d_6 \end{bmatrix}_{6\times 6} \tag{31}$$

If the matrix of $\boldsymbol{K}$ is nonsingular, that is $|\boldsymbol{K}| \neq 0$, Eq. (30) can be rewritten as

$$[\dot x\ \dot y\ \dot z\ \dot\phi_1\ \dot\phi_2\ \dot\phi_3]^T = \boldsymbol{J}[\dot\theta_1\ \dot\theta_2\ \dot\theta_3\ \dot\theta_4\ \dot\theta_5\ \dot\theta_6]^T \tag{32}$$

or

$$\dot{\boldsymbol{X}} = \boldsymbol{J}\dot\theta \tag{33}$$

where

$$\boldsymbol{J} = \boldsymbol{K}^{-1} \tag{34}$$

is the Jacobian matrix of the simplified 6-RUS parallel manipulators.

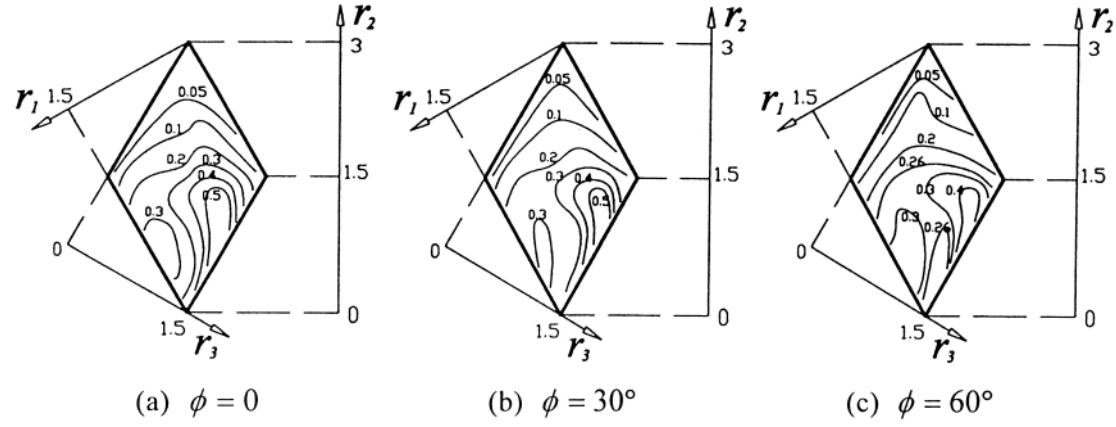

Fig. 11. Atlases of Global Torque Conditioning Index for 6-RUS Parallel Manipulator.

https://doi.org/10.1017/S0263574701003654 Published online by Cambridge University Press

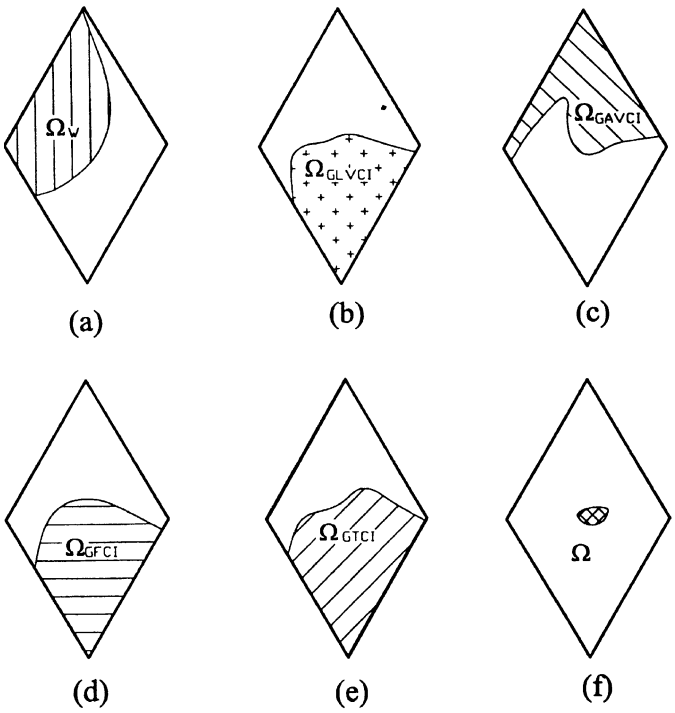

Fig. 12. The optimum regions of performance criteria in the physical model of the solution space for 6-RUS Parallel Manipulators.

6.2. Global conditioning indices

The accuracy of the control of the manipulator is dependent on the condition number of the Jacobian matrix.[25] This number is to be kept as small as possible. If the number can be unity, the matrix is an isotropic one, and the manipulator is in an isotropic configuration. The condition number is defined as[25]

$$\kappa_J = \| \boldsymbol{J} \| \, \| \boldsymbol{J}^{-1} \| \tag{35}$$

where $\| \cdot \|$ denotes any norm, e.g., Euclidean norm, of its matrix argument. Other definitions for the norm could be adopted. For instance, the square root of the largest eigenvalue of $\boldsymbol{J}^T \boldsymbol{J}$ is often used. This definition has the advantage of being applicable to non-square matrices.

From the standpoint of mathematics, the condition number of a matrix is used in numerical analysis to estimate the error generated in the solution of a linear system of equations by the error on the data.[26] From Eq. (33), one obtains,

$$\frac{\| \delta \dot{\theta} \|}{\| \dot{\theta} \|} \leq \kappa_J \frac{\| \delta \dot{\boldsymbol{X}} \|}{\| \dot{\boldsymbol{X}} \|} \tag{36}$$

When applied to manipulators, the elements of vector $\dot{\boldsymbol{X}}$ may have different dimensions. In this case, we cannot define the relative errors of $\| \delta \boldsymbol{X} \| / \| \boldsymbol{X} \|$. The definition of κ_J has indeterminate physical significance. From this context, we define the following isotropy indices.

6.2.1. Global Velocity Conditioning Indices (GVCI). For the reason of non-identical dimension, Eq. (32) can be rewritten as

$$\begin{bmatrix} \dot{x} \\ \dot{y} \\ \dot{z} \end{bmatrix} = [\boldsymbol{J}_V][\dot{\theta}_1 \;\; \dot{\theta}_2 \;\; \dot{\theta}_3 \;\; \dot{\theta}_4 \;\; \dot{\theta}_5 \;\; \dot{\theta}_6 \;]^T \tag{37}$$

$$\begin{bmatrix} \dot{\phi}_1 \\ \dot{\phi}_2 \\ \dot{\phi}_3 \end{bmatrix} = [\boldsymbol{J}_\omega][\dot{\theta}_1 \;\; \dot{\theta}_2 \;\; \dot{\theta}_3 \;\; \dot{\theta}_4 \;\; \dot{\theta}_5 \;\; \dot{\theta}_6 \;]^T \tag{38}$$

where

$$[\boldsymbol{J}] = \begin{bmatrix} \boldsymbol{J}_V \\ \hline \boldsymbol{J}_\omega \end{bmatrix} \tag{39}$$

Therefore, we define the indices as follows

$$\kappa_V = \| \boldsymbol{J}_V \| \, \| \boldsymbol{J}_V^+ \|, \;\; \kappa_\omega = \| \boldsymbol{J}_\omega \| \, \| \boldsymbol{J}_\omega^+ \| \tag{40}$$

and

$$1 \leq \kappa_V < \infty, \;\; 1 \leq \kappa_\omega < \infty \tag{41}$$

where $\boldsymbol{J}_V^+$, $\boldsymbol{J}_\omega^+$ are the generalized inverse matrix of $\boldsymbol{J}_V$ and $\boldsymbol{J}_\omega$ respectively, since the matrices $\boldsymbol{J}_V$ and $\boldsymbol{J}_\omega$ are not square matrix mostly. κ_V and κ_ω are used to evaluate for linear and angular velocity isotropy of manipulators.

As for the definition of the condition number, if the value of κ_V or κ_ω is large, the matrix $\boldsymbol{J}_V$ or $\boldsymbol{J}_\omega$ is an ill-conditioned one, and the Eq. (37) or Eq. (38) is an ill-conditioned equation; if the value is small, the corresponding matrix and equation are well-conditioned ones. When κ_V attains its minimum value of 1 ($\kappa_V = 1$), the corresponding configuration is called as linear velocity isotropy. And if κ_ω reaches its minimum value of 1 ($\kappa_\omega = 1$), the corresponding configuration is called an angular velocity isotropy.

κ_V and κ_ω are configuration-dependent, they are local performance indices which are called *local velocity isotropy indices (LVII)*. In order to evaluate the global behavior of a

Table I. One example of the design for spatial 6-RUS parallel manipulators.

Dimensions of 6-RUS Parallel Manipulator	Workspace Volume	GLVCI	GAVCI	GFCI	GTCI
$r_1 = 1.24$, $r_2 = 1.61$, $r_3 = 0.15$, $\phi = 40°$	13.2	0.23	0.034	0.46	0.31

https://doi.org/10.1017/S0263574701003654 Published online by Cambridge University Press

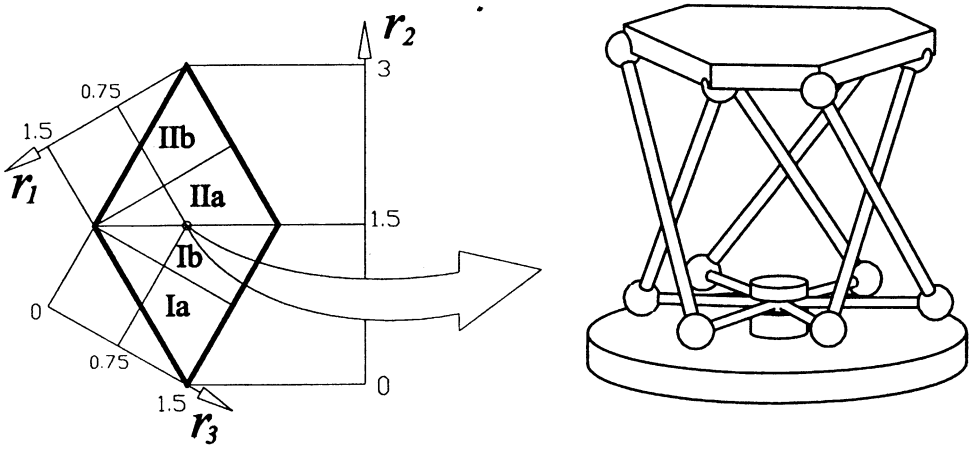

Fig. 13. One example of the design for spatial 6-RUS Parallel Manipulators ($r_1=r_3=0.75$, $r_2=1.5$, $\phi=40°$).

manipulator we define *global velocity conditioning indices (GYCI)* as follows:

$$\eta_V=\frac{\int_W \frac{1}{\kappa_V}\,dW}{\int_W dW}, \quad \eta_\omega=\frac{\int_W \frac{1}{\kappa_\omega}\,dW}{\int_W dW} \tag{42}$$

where W is the reachable workspace of the manipulator. η_V and η_ω are *global linear velocity conditioning index (GAVCI)* and *global angular velocity conditioning index (GAVCI)*, respectively. From Eq. (42), we can see that the values η_V and η_ω are the average values of $1/\kappa_V$ and $1/\kappa_\omega$ in the reachable workspace. In particular, a large value of the index ensures that the manipulator can be precisely controlled.

6.2.2. Global Force/Torque Conditioning Indices (GF/TCI). By virtue of what is called the *duality of kinematic and static*,[27] the forces and moments applied at the gripper under static conditions are related to the forces or moments required at the actuators to maintain the equilibrium by the transpose of the Jacobian matrix $\boldsymbol{J}$. This is also true for parallel manipulators,[8] and we can write

$$\tau=\boldsymbol{J}^T\begin{pmatrix}\boldsymbol{F}\\ \boldsymbol{M}\end{pmatrix} \tag{43}$$

where τ is the vector of actuator generalized force, and $\boldsymbol{F}$ and $\boldsymbol{M}$ are the external force and torque at the end effector, respectively. If $\boldsymbol{J}^T$ is a non-singular matrix, Eq. (43) can be rewritten as

$$\begin{pmatrix}\boldsymbol{F}\\ \boldsymbol{M}\end{pmatrix}=(\boldsymbol{J}^T)^{-1}\,\tau \tag{44}$$

where, matrix $(\boldsymbol{J}^T)^{-1}$ is called force Jacobian matrix which is noted as

$$\boldsymbol{G}=(\boldsymbol{J}^T)^{-1} \tag{45}$$

in another form

$$\boldsymbol{G}=\begin{pmatrix}\boldsymbol{G}_F\\ \boldsymbol{G}_M\end{pmatrix}=(\boldsymbol{J}^T)^{-1} \tag{44}$$

Then Eq. (44) can be rewritten as

$$\begin{pmatrix}\boldsymbol{F}\\ \boldsymbol{M}\end{pmatrix}=\begin{pmatrix}\boldsymbol{G}_F\\ \boldsymbol{G}_M\end{pmatrix}\tau \tag{47}$$

or

$$(\boldsymbol{F})=(\boldsymbol{G}_F)\,\tau \tag{48}$$

$$(\boldsymbol{M})=(\boldsymbol{G}_M)\,\tau \tag{49}$$

We define the force and torque isotropy indices as follows:

$$\kappa_F=\|\boldsymbol{G}_F\|\,\|\boldsymbol{G}_F{}^+\|, \quad \kappa_M=\|\boldsymbol{G}_M\|\,\|\boldsymbol{G}_M{}^+\| \tag{50}$$

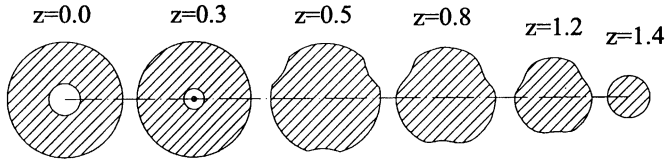

Fig. 14. Sections of the reachable workspace for the non-dimensional 6-RUS Parallel Manipulator $r_1=r_3=0.75$, $r_2=1.5$, $\phi=40°$.

https://doi.org/10.1017/S0263574701003654 Published online by Cambridge University Press

and

$$1 \le \kappa_F < \infty,\ 1 \le \kappa_M < \infty \tag{51}$$

where $\boldsymbol{G}_F{}^+$, $\boldsymbol{G}_M{}^+$ are the generalized inverse matrix of $\boldsymbol{G}_F$ and $\boldsymbol{G}_M$, respectively, since the matrices $\boldsymbol{G}_F$ and $\boldsymbol{G}_M$ are not square matrix. κ_F and κ_M are used to evaluate force and torque isotropy of manipulators.

Similarly, if the value of κ_F or κ_M is large, the matrix $\boldsymbol{G}_F$ or $\boldsymbol{G}_M$ is an ill-conditioned one, and the Eq. (48) or Eq. (49) is an ill-conditioned equation; if the value is small, the corresponding matrix and equation are well-conditioned ones. When κ_F attains its minimum value of 1 ($\kappa_F=1$), the corresponding configuration is called as force isotropy. And if κ_M reaches its minimum value of 1($\kappa_M=1$), the corresponding configuration is called as torque isotropy.

κ_F and κ_M are also configuration-dependent, they are local performance indices which are called *local force/torque isotropy indices (LF/TII)*. In order to evaluate the global behavior of a manipulator we define *global force/torque conditioning indices (GF/TCI)* as follows:

$$\eta_F = \frac{\int_W \frac{1}{\kappa_F} dW}{\int_W dW}, \quad \eta_M = \frac{\int_W \frac{1}{\kappa_M} dW}{\int_W dW} \tag{50}$$

where W is the reachable workspace of the manipulator. η_F and η_M are *global force conditioning index (GFCI)* and *global torque conditioning index (GTCI)*, respectively.

6.3. Atlases for global conditioning indices

Given the definition of the global conditioning indices, we can calculate the values of the indices for all spatial 6-RUS parallel manipulators in the physical model of the solution space as shown in Figure 3 when ϕ is specified. And the atlases for the global conditioning indices can be obtained as shown in Figures 8–11.

Figure 8 shows the atlases for the global linear velocity conditioning index, from which we can see that:

- The index value is basically proportional to r_3;
- Generally, the index value is inversely proportional to r_2;
- The value of global linear velocity conditioning index for a 6-RUS parallel manipulator, r_1, r_2 and r_3 being specified, changes little for various values of ϕ.

Figure 9 shows the atlases for the global angular velocity conditioning index, from which we can see that:

- The index value is basically proportional to r_2;
- For the manipulators in the region of $r_1 \le 0.75 \cup r_3 \ge 1.5$, the index values are larger than others;
- The value of global angular velocity conditioning index for a 6-RUS parallel manipulator, r_1, r_2 and r_3, being specified, changes little for various value of ϕ.

Figure 10 shows the atlases for the global force conditioning index. The distributing characteristics of the index in the physical model of the solution space are:

- The index value is basically proportional to r_3;
- The values of the global force conditioning index for 6-RUS parallel manipulators in the region of r_3 is large and $r_1 \approx 0.75$ are larger than the manipulators' in other regions;
- The value of the index for a 6-RUS parallel manipulator, r_1, r_2 and r_3 being specified, changes little for various value of ϕ.

Figure 11 shows the atlases for the global torque conditioning index. The distributing characteristics of the index in the physical model of the solution space are identical with that of the global force conditioning index.

7. RESULTS OF THE DESIGN FOR THE 6-RUS PARALLEL MANIPULATORS

From Figures 6 and 7, we can see that the manipulators, with large volumes of reachable workspaces, are located in region IIb, in which workspaces of the manipulators are characterized by presence of voids.

From the atlases of global conditioning indices, we can conclude that the influence to values of the indices from the angular parameter ϕ is little. And in region of $0.75 \le r_2 \le 1.5 \cup r_3 \ge 0.75$, the global conditioning indices of the manipulators are better, except for the global angular velocity conditioning index. Therefore, it is difficult for us to select a 6-RUS parallel manipulator whose global conditioning indices are all best.

It is also difficult for us to design a spatial 6-RUS parallel manipulator whose workspace and global conditioning indices are all best. As shown in Figure 6, the region where the volume is greater than 10.0, noted as Ω_W, is shown as the shaded region in Figure 12(a). The shaded region in Figure 12(b) is the region of the GLVCI being greater than 0.2, noted as Ω_{GLVCI}. Other regions of GAVCI > 0.03, GFCI > 0.3 and GTCI > 0.2 can also be obtained as shown the shaded regions in Figure 12(c), (d) and (e), which are denoted as Ω_{GAVCI}, Ω_{GFCI} and Ω_{GTCI}, respectively. Therefore, the designed manipulators considering all the criteria, such as workspace volume and the global conditioning indices, are within the region noted as Ω, as shown in Figure 12(f), which is the intersection of the regions mentioned above. For example, link lengths and values of the criteria of the manipulator $r_1=1.24$, $r_2=1.61$, $r_3=0.15$, $\phi=40°$, are shown in Table I. The architecture and the workspace of the manipulator are shown in Figures 13 and 14, respectively.

8. CONCLUSIONS

In this paper, a design method is proposed for the design of spatial 6-RUS parallel manipulators. The design method is based on the physical model of the solution space and performance atlases. The workspace, volume and shape, for the manipulators is studied systematically. Some global conditioning indices are defined to design the manipulators. The atlases for the workspace and the global conditioning indices are obtained and interpreted in the physical model of the solution space. The design results are presented. The technique of the optimal design used in this paper can be applied to the design of other manipulators.

https://doi.org/10.1017/S0263574701003654 Published online by Cambridge University Press

ACKNOWLEDGMENTS

This work was supported by the China Postdoctoral Science Foundation, the Tsinghua-Zhongda Postdoctoral Science Foundation, and the Mechanical Engineering School Academic Committee of Tsinghua University, respectively. The Hebei University of Technology is given due acknowledgment for the Foundation of 211 Project.

The authors would like to thank the anonymous reviewers for their detailed and pertinent comments.

References

1. K.C. Gupta, "On the Nature of Robot Workspace," *Int. J. Robotics Research* **5**, No. 2, 112–121 (1985).
2. A. Bajpai and B. Roth, "Workspace and mobility of a closed-loop manipulator," *Int. J. Robotics Research* **5**, No. 2, 131–142 (1986).
3. C.A. Klein and B.E. Blaho, "Dexterity Measures for the Design and Control of Kinematically Redundant Manipulators," *Int. J. Robotics Research* **6**, No. 2, 72–82 (1987).
4. J. Angeles and Lopez-Cajun C, "The dexterity index of serial-type robotic manipulators," *ASME Trends and Developments in Mechanisms, Machines and Robotics*, 79–84 (1988).
5. Feng Gao, Febrice Guy, and W.A. Gruver, "Criteria Based Analysis and Design of Three-Degree-of-Freedom Planar Robotic Manipulators," *Proceedings of the 1997 IEEE International Conference on Robotics and Automation*, New Mexico (April 1997) pp. 468–473.
6. C. Gosselin and J. Angeles, "A Global Performance Index for the Kinematic Optimization of Robotic Manipulators," *Transaction of the ASME, Journal of Mechanical Design* **113**, 220–226 (Sept. 1991).
7. Feng Gao, Xin-Jun Liu and W.A. Gruver, "Performance Evaluation of Two Degrees of Freedom Planar Parallel Robots," *Mechanisms and Machine Theory* **33**, No. 6, 661–668 (1998).
8. C. Gosselin, "Stiffness Map for Parallel Manipulators," *IEEE Transaction on Robotics and Automation* **6**, No. 3, 377–382 (June, 1990).
9. J.-P. Merlet, "MEMOCRAT: A design methodology for the conception of robots with parallel architecture," *Robotica* **15**, Part 4, 367–373 (1997).
10. M. Thomas, H.C. Yuan-Chou, and D. Tesar, "Optimal actuator sizing for robotic manipulators based on local dynamic criteria," *Journal of Mech., Trans., and Autom. in Design* **107**, 163–169 (1985).
11. Ji-Hou Yang and Feng Gao, "About the diagrams of max. and min. kinematic influence coefficients of four-bar mechanisms," *The 4th IFToMM, Inter. Sym. on Linkages and CAD Methods* **Vol. 1–1**, Paper 19, 141–152 (1985).
12. D. Stewart, "A Platform with 6 Degrees of Freedom," *Proc. of the Institution of Mechanical Engineers* **180**(1), 371–386 (1965).
13. H. MacCallion and D.T. Pham, "The Analysis of a Six Degrees of Freedom Work Station for Mechanized Assembly," *Proc. 5th World Congress on Theory of Machines and Mechanisms* (1979) 611–616.
14. E.F. Ficher, "A Stewart Platform-Based Manipulator: General Theory and Practical Construction," *Int. J. Robotics Research* **5**, No. 2, 157–182 (1986).
15. Z. Huang and H.B. Wang, "Dynamic Force Analysis of 6-DOF Parallel Multiloop Robot Manipulators," *ASME Paper 86-DEF-168* (1986).
16. M. Griffis and J. Duffy, "A Forward Displacement Analysis of a Class of Stewart Platforms," *J. Robotic Systems* **6**, No. 6, 703–720 (1989).
17. Z. Huang, Y.Y. Qu and Y.S. Zhao, "Special Configuration and its Properties of Spatial Parallel Manipulator 6-SPS Mechanisms," *Proc of 8th IFToMM World Congress on TMM* (1991) pp. 991–994.
18. Y.L. Chi, "Systems and Methods Employing a Rotary Track for Machining and Manufacturing," *WIPO Patent, No. WO99/38646* (1999).
19. Yukio Takeda, Hiroaki Funabashi and Hironobu Ichimaru, "Development of Spatial In-Parallel Actuated Manipulators with Six Degrees of Freedom with High Motion Transmissibility," *JSME International Journal Series C* **40**, No. 2, 299–308 (June, 1997).
20. Yukio Takeda, http://www.mech.titech.ac.jp/~youso/takeda/6-RSS(1998).htm (2000).
21. Masaru Uchiyama, http://www.space.mech.tohoku.ac.jp/research/hexa/hexa.jpg (2001).
22. ANCO Engineers, http://www.ancoengineers.com/photos/ancor156.html (2000).
23. Servos & Simulation, http://www.servos.com/6axis.html(2000).
24. I.A. Bonev and J. Ryu, "A Geometrical Method for Computing the Constant-Orientation Workspace of 6-PRRS Parallel Manipulators", *Mechanism and Machine Theory* **36**, No. 1, 1–13 (2001).
25. J.K. Salisbury and J.J. Craig, "Articulated Hands: Force Control and Kinematic Issues," *Int. J. Robot. Res.* **1**(1), 4–12 (1982).
26. G. Strang, "Linear Algebra and its Application (Academic Press, New York, 1976).
27. K.J. Waldron and K.H. Hunt, "Series-parallel Dualities in Actively Coordinated Mechanisms," *Int. J. Robotics Research* **4**, 175–181 (1988).